Published in final edited form as:
Liver Int. 2014 March ; 34(3): 427–437. doi:10.1111/liv.12353.

Mixed lineage kinase 3 deficient mice are protected against the high fat high carbohydrate diet-induced steatohepatitis

Samar H. Ibrahim[1], **Gregory J. Gores**[2], **Petra Hirsova**[2], **Michelle Kirby**[3], **Lili Miles**[4], **Anja Jaeschke**[5], and **Rohit Kohli**[3]

[1]Division of Pediatric Gastroenterology and Hepatology Mayo Clinic, College of Medicine, MN, USA

[2]Division of Gastroenterology and Hepatology, Mayo Clinic, College of Medicine, Rochester, MN, USA

[3]Division of Gastroenterology, Hepatology and Nutrition, Cincinnati Children's Hospital Medical Center, Cincinnati, Ohio, USA

[4]Department of Pathology, Cincinnati Children's Hospital Medical Center, Cincinnati, Ohio, USA

[5]Department of Pathology and Laboratory Medicine, University of Cincinnati College of Medicine, Cincinnati, Ohio, USA

Abstract

Background—C-Jun N-terminal kinase (JNK) activation is pivotal in the development of nonalcoholic steatohepatitis (NASH). Mixed lineage kinase 3 (MLK) 3 is one of the mitogen activated protein kinase kinase kinase (MAP3K) that mediates JNK activation in the liver. Despite this concept, the role of MLK3 in modulating liver injury during nutrient excess has not been explored.

Aims—our aim was to determine if MLK3 deficient mice were protected against high fat high carbohydrate (HFHC) diet-induced NASH.

Methods—We employed eight-week-old *Mlk3*$^{-/-}$ male C57BL/6J mice, and wild type (WT) mice C57BL/6J as controls. Mice were fed a HFHC or a chow diet adlib for 16 weeks.

Results—Hepatic JNK activating phosphorylation was readily absent in the *Mlk3*$^{-/-}$ mice fed the HFHC diet, but not in WT mice. This inhibition of JNK activation was hepatoprotective. Despite a comparable increase in weight gain, hepatic steatosis by histological examination and hepatic triglyceride quantification was reduced in HFHC diet-fed *Mlk3*$^{-/-}$ mice compared to WT mice. In addition, compared to the WT mice, HFHC diet-fed *Mlk3*$^{-/-}$ mice had significantly attenuated liver injury as manifested by reduced ALT levels, hepatocyte apoptosis, markers of hepatic inflammation, and indices of hepatic fibrogenesis.

Address for correspondence: Rohit Kohli, MBBS, MS, Associate Professor of Pediatrics, Co-Director Cincinnati Children's Steatohepatitis Center, Cincinnati Children's Hospital Medical Center, 3333 Burnet Avenue,, Cincinnati, Ohio 45229-3026, Tel: (513) 803-0908, Fax: (513) 803-2785, Rohit.Kohli@cchmc.org.

Disclosure: The authors have no potential conflict of interest in regards to this manuscript.

Conclusion—our results suggest that loss of MLK3 in mice is protective against HFHC diet-induced NASH, in a weight-independent fashion, through attenuation of JNK activation. MLK3 is a potential therapeutic target for the treatment of human NASH.

Keywords

JNK; lipoapoptosis; nonalcoholic fatty liver disease; inflammation; fibrosis

INTRODUCTION

Nonalcoholic fatty liver disease (NAFLD) is an evolving public health problem linked to the epidemic of obesity, and its associated insulin resistance and diabetes (1). Up to 30% of the western population is affected by NAFLD (2). A significant subset of these patients develops nonalcoholic steatohepatitis (NASH), the more severe form of the disease. NASH is characterized by hepatocyte apoptosis, hepatic infiltration by inflammatory cells and fibrosis. Individuals with NASH can progress to cirrhosis with its sequelae including the development of end-stage liver disease and hepatocellular carcinoma (3). Thus, the cellular and molecular mechanisms promoting liver injury in NASH are of both biomedical and public health interest.

Liver injury in NASH is in part mediated by lipids and hence NASH is a lipotoxic disorder. In particular, as excess of toxic saturated free fatty acids (SFAs) are present in the circulation in this disorder (4). SFAs signal nefarious intracellular signaling cascades mediating inflammation and hepatocytes apoptosis (5, 6). C-Jun N-terminal kinase (JNK) is activated in both the macrophages and hepatocytes in this disorder causing apoptosis and liver injury (7, 8). JNK belongs to a family of mitogen-activated protein kinases (MAPKs); of three known JNK genes, JNK1 and JNK2 are expressed in the liver (9). JNK activation is essential in both the metabolic syndrome associated with NAFLD and cellular apoptosis. JNK is activated in murine dietary and genetic models of NASH (10–12), and also in human NASH (13, 14). In mice models of genetic and dietary obesity JNK phosphorylates insulin receptor substrate-1, suppressing insulin receptor signaling, and inducing insulin resistance (15). Both JNK1 and JNK2 have been implicated in insulin resistance, although JNK1 is more strongly associated with steatohepatitis (11, 12). In a mouse model of obesity, absence of JNK1 results in decreased adiposity, and significant improvement of insulin sensitivity (10). Liver specific knockdown of JNK1 in obese mice lowers blood glucose and insulin levels, but interestingly, increases triglyceride (TG) level (16). In contrast, high fat diet-fed *Jnk2*$^{-/-}$ mice were obese, insulin-resistant, and had increased liver injury. On the other hand, antisense oligonucleotide knockdown of JNK2 improved insulin sensitivity but had no effect on hepatic steatosis and markedly increased liver injury (12). However the upstream kinases activating JNK in NASH remain poorly characterized.

The mixed lineage kinases (MLK)s are a family of serine/threonine protein kinases that function in a phospho relay module to control the activity of specific MAPKs. Members of the family include MLK1, MLK2, MLK3, dual leucine zipper-bearing kinase, and leucine zipper-bearing kinase (17). MAPKs are a group of protein serine/threonine kinases that are activated in response to a wide variety of external stress signals and mediate signal

transduction cascades that play an important regulatory role in cell growth, differentiation, and apoptosis (18). Many of these protein kinases are expressed in only a limited number of tissues, however MLK3 is the member of this gene family that is ubiquitously expressed (19). MLK3 has been implicated in multiple signaling cascades, including the NF-kappaB pathway, the extracellular signal-regulated kinase, JNK, and p38 MAPK pathways (17, 20, 21). Previous studies have demonstrated that MLK3 is the MAP3K that mediates SFAs induced JNK activation (22, 23), and absence of inositol requiring enzyme 1 alpha (IRE1α) one of the stress-sensing endoplasmic reticulum (ER) resident protein, and apoptosis regulating kinase 1 (ASK1) one of the MAP3K isoforms do not inhibit SFA induced JNK activation (23). However the role of MLK3 in modulating hepatocyte apoptosis, hepatic fibrosis and inflammation in vivo remains unexplored.

Herein, we observed that Mlk3 genetic deficiency in a murine nutritional model of diet induced obesity, insulin resistance and NASH has a beneficial effect on the disease progression by decreasing liver steatosis, injury, inflammation and fibrosis. We observed a reduction in liver cells apoptosis and macrophage-associated hepatic inflammation. These effects were accompanied by a reduction in hepatic activating phosphorylation of JNK. We speculate that MLK3 is a potential therapeutic target for the treatment of human NASH.

MATERIALS AND METHODS

Animals and diets

The Institutional Animal Care and Use Committee at the University of Cincinnati approved the animal studies. All animals received humane care. Adult wild type (WT) male C57Bl/6 mice (Jackson Laboratory, Bar Harbor, ME) and *Mlk3*$^{-/-}$ male C57Bl/6 mice (19) were group-housed 2–3/cage (22 ± 2°C) on a 12-hour light-dark cycle. 6 to 9 animals per group were randomized to either chow (Teklad-Harlan, Madison, WI), or high fat high carbohydrate (HFHC) diet from OpenSource diets D123311 with 58% of calories from fat and drinking water with high fructose (55% fructose; Acros Organics, Morris Plains, NJ) and sucrose (45% sucrose; Sigma-Aldrich, St. Louis, MO) at a concentration of 42 g/L (24). Animals were provided ad-lib access to diets for 16 weeks. Body weights and food intake were recorded. Blood samples were collected from the tail vein after an overnight fast after 7, and 15 weeks on the diet and at time of sacrifice via cardiac puncture. Fasting blood glucose concentrations were measured with One Touch Glucometer (LifeScan, Milpitas, CA), and plasma insulin was measured by ELISA kit for mice insulin (Crystal Chem. Inc., IL). Harvested livers were removed and rapidly frozen in liquid nitrogen for biochemical analysis. Histology was performed using tissue fixed in 10% formalin, dehydrated, and embedded in paraffin. Sections were stained with hematoxylin and eosin, and Sirius red stain.

Genotype analysis

The wild-type (140-bp) and disrupted (275-bp) alleles of *Mlk3* were detected by PCR amplification of genomic DNA using the primers 5′-AGCAAACTCCGAGCAAGGGAC-3′, 5′-GGCTAAACCAGAACTCAAGCGTG-3′, and 5′-GTAGAAGGTGGCGCGAAGGG-3′. PCR products were separated by agarose gel electrophoresis for genotyping.

Hepatic triglyceride (TG) and serum alanine aminotransferase (ALT) quantification

Hepatic TG content was determined from mouse liver homogenates as previously described (24). Briefly, 100 milligrams of wet liver tissue were homogenized in a 20 mM Tris buffer. Triglyceride reagent set (Pointe Scientific, Canton, MI) was used for the assay per manufacturer's instructions. Photometric absorbance was read at 500 nm using Synergy 2 microplate reader (BioTek, Winooski, VT). ALT was measured from mouse serum utilizing DiscretPak™ ALT Reagent Kit (Catachem, Bridgeport, CT). ALT enzyme kinetics was measured over a five minute interval by measuring change in photometric absorbance at 340 nm.

Real-time polymerase chain reaction (PCR)

Liver total RNA was extracted from the liver tissues using RNeasy Plus Kit (Qiagen, Valencia, CA) and was reverse-transcribed into complementary DNA with Moloney leukemia virus reverse transcriptase and random primers (both from Invitrogen, Grand Island, NY). Quantification of the complementary DNA template was performed with real-time PCR (Light Cycler 480; Roche Applied Science, Indianapolis, IN) using SYBR green (Molecular Probes, Roche, Indianapolis, IN) as a fluorophore using the mouse primers listed in Table 1.

Western blotting

Liver protein extracts were prepared using Triton lysis buffer [20 mM Tris (pH 7.4), 1% Triton X-100, 10% glycerol, 137 mM NaCl, 2 mM EDTA, 25 mM β-glycerophosphate, 1 mM sodium orthovanadate, 1 mM phenylmethyl sulfonyl fluoride, and 10 μg/mL of aprotinin and leupeptin]. Extracts (50 μg of protein) were examined by immunoblot analysis, loaded onto SDS-polyacrylamide gel (Invitrogen, Carlsbad, CA, USA) were probed for phosphorylated C-Jun N-terminal kinase (JNK-P) (# 9251), total JNK (# 9252) (Cell Signaling Technology, Beverly, MA), β-actin (Santa Cruz Biotechnology, Santa Cruz, CA) using standard western blotting methods. Primary antibodies were used at a dilution of 1:1000. Appropriate horseradish peroxidase-conjugated secondary antibodies (Biosource International, Camarillo, CA) were used at a dilution of 1:3000.

Quantification of apoptosis, fibrosis and macrophage infiltration

Apoptotic cells were quantified in paraffin-embedded hepatic tissue by chromogenic method using the Apop Tag Peroxidase in Situ Apoptosis Detection Kit from Millipore (Billerica, MA) that detects apoptotic cells in situ by labeling DNA strand breaks by the terminal deoxynucleotidyl transferase-mediated deoxyuridine triphosphate nick-end labeling (TUNEL) method as per the manufacturer's instructions. Diaminobenzidine was used as a peroxidase substrate (Vector Laboratories, Burlingame, CA); nuclear fast red was used for the counterstain. Apoptotic nuclei were quantified by counting nuclei in 10 random microscopic 20 × fields per animal using light microscopy (Eclipse Meta Morph V 5.0.7, Nikon, West Lafayette, IN), the averages of apoptotic nuclei were expressed as fold increase over control chow-fed WT mice, which was arbitrary set at 1. Liver fibrosis was quantified using Sirius red staining of paraformaldehyde-fixed paraffin-embedded liver tissue sections

after deparaffinization and hydration (25). Direct red 80 and Fast-green FCF (color index 42053) were obtained from Sigma-Aldrich Diagnostics.

Liver sections were stained with Sirius red stain, and red-stained collagen fibers were quantified by digital image analysis of ten random 20 × fields per animal using the ImageJ software (NIH), Sirius red-stained area in the liver tissue sections were averaged and normalized to control chow-fed WT animals, which was arbitrary, set at 1. Quantification of macrophage infiltration was done by immunohistochemistry. Paraformaldehyde-fixed paraffin-embedded liver tissue sections were deparaffinized, hydrated and incubated with Mac-2 antibody (eBioscience, San Diego, CA) used at a dilution of 1:250. Bound antibodies were detected using Vectastain ABC kit and diaminobenzidine as a substrate (both from Vector Laboratories, Burlingame, CA); the tissue sections were counterstained with methyl green. To quantify Mac-2 immunohistochemical staining, ten random 20 × fields per animal were assessed by morphometry (KS 400 software, Carl Zeiss).

Statistical Analysis

Results are expressed as mean ± SEM. Where indicated, the statistical significance between two groups was estimated by Student's t test or among three or more groups using ANOVA, with Bonferroni posttest correction for multiple comparisons. *, **, ***, indicate statistical significance with $p < 0.05$, $p < 0.01$, and $p < 0.001$, respectively. Statistically non-different results were labeled NS where appropriate. All analyses were performed using GraphPad Prism 6.0 software (San Diego, CA).

RESULTS

HFHC-fed *Mlk3*$^{-/-}$ mice have reduced JNK activation

Eight-week-old *Mlk3*$^{-/-}$ male C57BL/6J mice (Figure 1A) and WT mice C57BL/6J, employed as controls, were fed either chow diet or high fat high carbohydrate (HFHC) diet ad libitum for 16 weeks to induce NASH (24). The weight of mice fed HFHC diet was similar in the *Mlk3*$^{-/-}$ mice and wild type mice (Figure 1B). Caloric intake was not different between the groups (Figure 1C), neither the glucose nor the insulin tolerance tests (data not shown). Given the pivotal role of JNK in NASH, we next assessed JNK activation in HFHC diet-fed mice. JNK phosphorylation was significantly reduced in *Mlk3*$^{-/-}$ mice compared to the WT mice (Figure 1D). These data demonstrate that JNK activation was remarkably reduced in the HFHC diet-fed *Mlk3*$^{-/-}$ mice compared to WT mice, independent of body weight.

Mlk3$^{-/-}$ mice are protected against HFHC diet-induced steatosis and liver injury

Histological examination of hematoxylin and eosin-stained liver sections from WT and *Mlk3*$^{-/-}$ mice fed HFHC diet for 16 weeks (Figure 2A) revealed a significantly lower steatosis score in the *Mlk3*$^{-/-}$ mice compared to the WT mice (0.4 ± 0.2 vs 1.6 ± 0.4, $p = 0.03$) (Figure 2B) (26). Likewise, biochemical quantification of hepatic neutral TG was significantly lower in the HFHC fed *Mlk3*$^{-/-}$ mice, compared to the WT mice (692 ± 96 vs 1707 ± 363 mg/100 milligrams liver weight, $p = 0.03$) (Figure 2C). As hepatocyte apoptosis is a histopathological hallmark of NASH (27), we next examined apoptosis in liver tissue

samples using a TUNEL-based method. WT mice on the HFHC diet had a 3.2 fold increase in liver apoptotic cells vs 1.3 fold increase in liver apoptotic cells in the *Mlk3*$^{-/-}$ animals on the HFHC diet when normalized to the chow-fed WT control ($p = 0.04$) (Figure 3A & B). Consistent with the reduction in liver apoptotic cells, *Mlk3*$^{-/-}$ mice displayed reduced serum ALT values compared to WT HFHC diet-fed mice (49 ± 2 vs 96 ± 19 U/L, $p = 0.02$) (Figure 3C). Taken together, these data suggest that the *Mlk3*$^{-/-}$ mice were protected against HFHC diet-induced hepatic steatosis and liver injury.

Mlk3$^{-/-}$ mice are protected against HFHC diet-induced hepatic macrophage infiltration and activation

A growing body of evidence suggests that influx and activation of macrophages within the liver is an essential pathogenic element in the progression of NAFLD (28). We have previously shown that the HFHC diet results in macrophage activation in WT mice (24). Therefore, we examined hepatic macrophage markers in our current paradigm. We observed a significant increase in hepatic mRNA expression of macrophage surface markers in the HFHC diet-fed WT mice, but not in the *Mlk3*$^{-/-}$ mice on the same diet, when normalized to chow-fed WT mice [3.5 ± 0.5 fold vs 1.8 ± 0.4 fold, $p = 0.03$ for cluster of differentiation (CD)68; 2.2 ± 0.3 fold vs 0.7 ± 0.1 fold, $p = 0.004$ for F4/80; and 3.3 ± 0.7 fold vs 1.3 ± 0.2 fold, $p = 0.03$ for CD14] (Figure 4A). The considerable accumulation of hepatic macrophages in the HFHC-fed animals as compared to the chow-fed animals was confirmed by quantification of Mac-2 binding protein immunohistochemistry, a marker for phagocytically active macrophages, and was significantly reduced in the HFHC-fed *Mlk3*$^{-/-}$ mice compared to the WT mice when normalized to chow fed WT mice (3.3 ± 0.2 fold vs 2.1 ± 0.4 fold, $p < 0.05$) (Figure 4B). Moreover, evidence for macrophage activation was examined by determining hepatic mRNA expression of interleukin (IL)-1β, and monocyte chemotactic protein-1 (MCP-1), and tumor necrosis factor (TNF)α (Figure 4C). Indeed, hepatic mRNA for these cytokines and chemokines known to be secreted by activated macrophages were elevated in HFHC diet-fed WT mice, and reduced in the *Mlk3*$^{-/-}$ mice on the same diet when normalized to chow fed WT mice (3.3 ± 0.8 fold vs 0.8 ± 0.1 fold, $p = 0.02$ for IL-1β; 4.1 ± 1.1 fold vs 1 ± 0.2 fold, $p = 0.02$ for MCP-1; and 0.8 ± 0.1 vs 1.7 ± 0.2 fold, $p=0.009$ for TNFα). Collectively, these observations suggest that HFHC-fed *Mlk3*$^{-/-}$ mice are protected against liver injury by reducing infiltration and activation of hepatic macrophages.

Mlk3$^{-/-}$ mice are protected against HFHC diet-induced hepatic fibrosis

Hepatic fibrosis is the ominous sequela of chronic liver inflammation, leading to irreversible cirrhosis and end-stage liver disease (29). Hence, we next examined the protective effect of *Mlk3*$^{-/-}$ on the development of HFHC diet-induced hepatic fibrogenesis (24, 30). Osteopontin, a profibrogenic extracellular matrix protein and cytokine (31), α smooth muscle actin (αSMA) and collagen 1a1 mRNA levels, markers of activated hepatic stellate cells (32), are all up-regulated by the HFHC diet in the WT mice, whereas this up-regulation of the fibrogenesis gene is attenuated in the *Mlk3*$^{-/-}$ mice on the same diet when normalized to chow-fed WT mice (1.7 ± 0.2 fold vs 0.9 ± 0.1 fold, $p = 0.01$ for osteopontin; 2.7 ± 0.5 fold vs 1 ± 0.3 fold, $p = 0.03$ for αSMA ; 2.3 ± 0.4 fold vs 0.8 ± 0.1 fold, $p = 0.01$ for collagen 1a1) (Figure 5A). To assess deposition of excessive collagen matrix, liver sections

were stained with Sirius red stain. Liver sections from mice fed the HFHC diet had a significantly increased area of collagen deposition in the WT mice compared to the *Mlk3*$^{-/-}$ mice on the same diet when normalized to chow-fed WT mice (3.3 ± 0.6 fold vs 0.8 ± 0.1 fold, p = 0.01) (Fig. 5B & C). Collectively these data suggest that *Mlk3*$^{-/-}$ mice are protected against HFHC diet-induced hepatic fibrogenesis.

DISCUSSION

The principal findings of the present study provide mechanistic insights regarding the protective effect of *Mlk3* knockout in a murine nutritional model of NASH. Our results indicate that *Mlk3*$^{-/-}$ convey several salutary effects in the progression of NASH including: (i) inhibition of JNK phosphorylation, (ii) a decrease in hepatocyte injury and steatosis; and (iii) a reduction in hepatic markers of macrophage aggregation and activation, and inhibition of hepatic fibrogenesis. These observations are independent of obesity generated by the HFHC diet and are more thoroughly discussed below.

In this study we used a previously established ad libitum dietary model that resulted in NASH with fibrosis in non-genetically modified obese mice (24). Herein mice were fed a high fat (HF) diet and given ad libitum access to fructose in their drinking water. Compared to the mice fed the HF diet only, HFHC diet-fed mice had increased hepatic oxidative stress, macrophage aggregation in the liver, transforming growth factor β1-driven fibrogenesis and collagen deposition; while weight gain, body fat, insulin resistance and liver steatosis were similar between the two groups. Thus, fructose consumption was found to be necessary to move the process from simple steatosis to fibrogenesis (24). Interestingly we demonstrated that the *Mlk3*$^{-/-}$ mice on the same HFHC diet have a relative attenuation of all the injurious features of NASH in this model without an impact on overall obesity. In concurrence with our findings, in a previous study *Mlk3*$^{-/-}$ mice on HF diet had significantly reduced hepatic steatosis compared to the WT mice on the same diet, without change in insulin or glucose tolerance. In our current study, we advance these observations by demonstrating that *Mlk3*$^{-/-}$ mice on HFHC diet had significantly reduced hepatocyte apoptosis, macrophage activation, and hepatic fibrogenesis compared to WT mice on the same diet independent of weight gain. Taken together, these results imply an important role of the MLK3 signaling pathway in the pathogenesis of NASH, an observation that is consistent with the activation of MLK3 by HF diet and parallels histological changes typical of NASH in mice (22).

SFA-induced JNK activation has been well documented in both rodent and human steatohepatitis (8, 12, 13, 33). As expected HFHC diet-fed WT mice have increased JNK phosphorylation, which was reduced in the *Mlk3*$^{-/-}$ mice on the same diet. MLK3 has been implicated in the activation of apoptotic cell death secondary to various stressful stimuli in neuronal, ovarian, pancreatic and hepatoma cells (17, 21, 34–36), on the other hand, hepatocytes depleted of MLK3 were partially protected from SFA-induced apoptosis (23), a prominent feature of NASH (13, 27, 37, 38). Consistent with the human disease, serum ALT and TUNEL-positive liver cells were increased in mice fed the HFHC diet. However *Mlk3*$^{-/-}$ mice had significantly reduced serum ALT and TUNEL-positive liver cells. Thus, MLK3 deficiency may reduce HFHC-induced hepatocytes injury in vivo by inhibiting JNK activation.

Macrophages have been implicated as central players in the inflammatory component of insulin resistance in the liver (24, 39, 40). Therefore, we examined markers for macrophages and their activation status in HFHC diet-fed WT and *Mlk3*$^{-/-}$ mice. Consistent with other studies (24, 41), mice fed the HFHC diet displayed increased expression of macrophage markers in the liver including CD14, CD68, and F4/80 and more abundant Mac-2-positive cells. The macrophages appeared to be activated as TNFα, IL-1β, and MCP-1 were also increased in the mice on the HFHC diet. This increase in macrophage markers and aggregation was reduced in the *Mlk3*$^{-/-}$ mice, and might be attributed to attenuated liver injury secondary to reduced JNK-mediated apoptosis (8), JNK dependent differentiation of pro-inflammatory macrophages (42) and likely other mechanisms. Previous study has shown that MLK3 deficiency caused a selective reduction in TNFα-stimulated JNK activation in vitro (19); on the other hand, MLK3 was required for lipopolysaccharide induced TNFα expression (43). Taken together, these data raise the possibility of direct interaction between MLK3 and TNFα, leading to a feed forward mechanism for their activation process. The role of bone marrow-derived macrophages in this process has been recently explored; MLK3 was required for SFA-induced JNK activation, and proinflammatory polarization in macrophages (Anja Jaeschke, University of Cincinnati, personal communication).

In summary, our data extend prior observations regarding MLK3 pathway activation in liver injury (22, 44) by demonstrating a salutary effect of MLK3 knockout in a preclinical model of NASH pathogenesis. Given the protective effect of *Mlk3*$^{-/-}$ in our murine dietary model of NASH that is phenotypically close to the human disease, we speculate that pharmacological inhibitors of the MLK3 signaling pathway could have a potential therapeutic role in human NAFLD.

ACKNOWLEDGMENT

We thank Dr. Roger Davis, Howard Hughes Medical Institute Investigator at University of Mass Medical School for providing the *Mlk3*$^{-/-}$ mice, and for Courtney N. Hoover for providing excellent secretarial support.

Grants: This work was supported by NIH Grants DK41876 to GJG, DK08505 to RK, DK082583 to AJ the Mayo Foundation, Cincinnati Children's Hospital Medical Center and the University of Cincinnati.

Abbreviations

NAFLD	Nonalcoholic fatty liver disease
NASH	nonalcoholic steatohepatitis
SFAs	saturated free fatty acids
JNK	C-Jun N-terminal kinase
MAPKs	mitogen-activated protein kinases
TG	triglycerides
MLK	mixed lineage kinase
MAP3K	mitogen activated protein kinase kinase kinase
IRE1α	inositol requiring enzyme 1 alpha

ER	endoplasmic reticulum
ASK1	apoptosis regulating kinase 1
TG	triglyceride
WT	wild type
HFHC	high fat high carbohydrate
ALT	alanine aminotransferase
PCR	polymerase chain reaction
TUNEL	terminal deoxynucleotidyl transferase-mediated deoxyuridine triphosphate nick-end labeling
Mac-2	macrophage galactose-specific lectin
CD	cluster of differentiation
IL-1β	interleukin-1 beta
MCP-1	monocyte chemotactic protein-1
TNFα	tumor necrosis factor alpha
αSMA	alpha smooth muscle actin
HF	high fat

REFERENCES

1. Parekh S, Anania FA. Abnormal lipid and glucose metabolism in obesity: implications for nonalcoholic fatty liver disease. Gastroenterology. 2007; 132(6):2191–2207. [PubMed: 17498512]
2. Browning JD, Szczepaniak LS, Dobbins R, et al. Prevalence of hepatic steatosis in an urban population in the United States: impact of ethnicity. Hepatology. 2004; 40(6):1387–1395. [PubMed: 15565570]
3. Adams LA, Lymp JF, St Sauver J, et al. The natural history of nonalcoholic fatty liver disease: a population-based cohort study. Gastroenterology. 2005; 129(1):113–121. [PubMed: 16012941]
4. Sanyal AJ, Campbell-Sargent C, MIRSHAHI F, et al. Nonalcoholic steatohepatitis: association of insulin resistance and mitochondrial abnormalities. Gastroenterology. 2001; 120(5):1183–1192. [PubMed: 11266382]
5. Kusminski CM, Shetty S, Orci L, Unger RH, Scherer PE. Diabetes and apoptosis: lipotoxicity. Apoptosis : an international journal on programmed cell death. 2009; 14(12):1484–1495. [PubMed: 19421860]
6. Unger RH, Orci L. Lipoapoptosis: its mechanism and its diseases. Biochimica et biophysica acta. 2002; 1585(2–3):202–212. [PubMed: 12531555]
7. Kodama Y, Kisseleva T, Iwaisako K, et al. c-Jun N-terminal kinase-1 from hematopoietic cells mediates progression from hepatic steatosis to steatohepatitis and fibrosis in mice. Gastroenterology. 2009; 137(4):1467–1477. e5. [PubMed: 19549522]
8. Malhi H, Bronk SF, Werneburg NW, Gores GJ. Free fatty acids induce JNK-dependent hepatocyte lipoapoptosis. Journal of Biological Chemistry. 2006; 281(17):12093–12101. [PubMed: 16505490]
9. Johnson GL, Nakamura K. The c-jun kinase/stress-activated pathway: regulation, function and role in human disease. Biochim Biophys Acta. 2007; 1773(8):1341–1348. [PubMed: 17306896]
10. Hirosumi J, Tuncman G, Chang L, et al. A central role for JNK in obesity and insulin resistance. Nature. 2002; 420(6913):333–336. [PubMed: 12447443]

11. Schattenberg JM, Singh R, Wang Y, et al. JNK1 but not JNK2 promotes the development of steatohepatitis in mice. Hepatology. 2006; 43(1):163–172. [PubMed: 16374858]
12. Singh R, Wang Y, Xiang Y, Tanaka KE, Gaarde WA, Czaja MJ. Differential effects of JNK1 and JNK2 inhibition on murine steatohepatitis and insulin resistance. Hepatology. 2009; 49(1):87–96. [PubMed: 19053047]
13. Puri P, Mirshahi F, Cheung O, et al. Activation and dysregulation of the unfolded protein response in nonalcoholic fatty liver disease. Gastroenterology. 2008; 134(2):568–576. [PubMed: 18082745]
14. Cazanave SC, Mott JL, Elmi NA, et al. JNK1-dependent PUMA expression contributes to hepatocyte lipoapoptosis. J Biol Chem. 2009; 284(39):26591–26602. [PubMed: 19638343]
15. Ozcan U, Cao Q, Yilmaz E, et al. Endoplasmic reticulum stress links obesity, insulin action, and type 2 diabetes. Science. 2004; 306(5695):457–461. [PubMed: 15486293]
16. Yang R, Wilcox DM, Haasch DL, et al. Liver-specific knockdown of JNK1 up-regulates proliferator-activated receptor gamma coactivator 1 beta and increases plasma triglyceride despite reduced glucose and insulin levels in diet-induced obese mice. J Biol Chem. 2007; 282(31): 22765–22774. [PubMed: 17550900]
17. Kim KY, Kim BC, Xu Z, Kim SJ. Mixed lineage kinase 3 (MLK3)-activated p38 MAP kinase mediates transforming growth factor-beta-induced apoptosis in hepatoma cells. The Journal of biological chemistry. 2004; 279(28):29478–29484. [PubMed: 15069087]
18. Robinson MJ, Cobb MH. Mitogen-activated protein kinase pathways. Current opinion in cell biology. 1997; 9(2):180–186. [PubMed: 9069255]
19. Brancho D, Ventura JJ, Jaeschke A, Doran B, Flavell RA, Davis RJ. Role of MLK3 in the regulation of mitogen-activated protein kinase signaling cascades. Mol Cell Biol. 2005; 25(9): 3670–3681. [PubMed: 15831472]
20. Chadee DN, Kyriakis JM. MLK3 is required for mitogen activation of B-Raf, ERK and cell proliferation. Nature Cell Biology. 2004; 6(8):770–776.
21. Xu Z, Maroney AC, Dobrzanski P, Kukekov NV, Greene LA. The MLK family mediates c-Jun N-terminal kinase activation in neuronal apoptosis. Molecular and cellular biology. 2001; 21(14): 4713–4724. [PubMed: 11416147]
22. Jaeschke A, Davis RJ. Metabolic stress signaling mediated by mixed-lineage kinases. Mol Cell. 2007; 27(3):498–508. [PubMed: 17679097]
23. Sharma M, Urano F, Jaeschke A. Cdc42 and Rac1 are major contributors to the saturated fatty acid-stimulated JNK pathway in hepatocytes. Journal of hepatology. 2012; 56(1):192–198. [PubMed: 21703174]
24. Kohli R, Kirby M, Xanthakos SA, et al. High-fructose, medium chain trans fat diet induces liver fibrosis and elevates plasma coenzyme Q9 in a novel murine model of obesity and nonalcoholic steatohepatitis. Hepatology. 2010; 52(3):934–944. [PubMed: 20607689]
25. Canbay A, Higuchi H, Bronk SF, Taniai M, Sebo TJ, Gores GJ. Fas enhances fibrogenesis in the bile duct ligated mouse: A link between apoptosis and fibrosis. Gastroenterology. 2002; 123(4): 1323–1330. [PubMed: 12360492]
26. Kleiner DE, Brunt EM, Van Natta M, et al. Design and validation of a histological scoring system for nonalcoholic fatty liver disease. Hepatology. 2005; 41(6):1313–1321. [PubMed: 15915461]
27. Feldstein AE, Canbay A, Angulo P, et al. Hepatocyte apoptosis and fas expression are prominent features of human nonalcoholic steatohepatitis. Gastroenterology. 2003; 125(2):437–443. [PubMed: 12891546]
28. Baffy G. Kupffer cells in non-alcoholic fatty liver disease: the emerging view. Journal of hepatology. 2009; 51(1):212–223. [PubMed: 19447517]
29. Ekstedt M, Franzen LE, Mathiesen UL, et al. Long-term follow-up of patients with NAFLD and elevated liver enzymes. Hepatology. 2006; 44(4):865–873. [PubMed: 17006923]
30. Charlton M, Krishnan A, Viker K, et al. Fast food diet mouse: novel small animal model of NASH with ballooning, progressive fibrosis, and high physiological fidelity to the human condition. American journal of physiology Gastrointestinal and liver physiology. 2011; 301(5):G825–G834. [PubMed: 21836057]

31. Syn WK, Choi SS, Liaskou E, et al. Osteopontin is Induced by Hedgehog Pathway Activation and Promotes Fibrosis Progression in Nonalcoholic Steatohepatitis. Hepatology. 2011; 53(1):106–115. [PubMed: 20967826]
32. Friedman SL. Molecular regulation of hepatic fibrosis, an integrated cellular response to tissue injury. The Journal of biological chemistry. 2000; 275(4):2247–2250. [PubMed: 10644669]
33. Wang Y, Ausman LM, Russell RM, Greenberg AS, Wang XD. Increased apoptosis in high-fat diet-induced nonalcoholic steatohepatitis in rats is associated with c-Jun NH2-terminal kinase activation and elevated proapoptotic Bax. J Nutr. 2008; 138(10):1866–1871. [PubMed: 18806094]
34. Cole ET, Zhan Y, Abi Saab WF, Korchnak AC, Ashburner BP, Chadee DN. Mixed lineage kinase 3 negatively regulates IKK activity and enhances etoposide-induced cell death. Biochim Biophys Acta. 2009; 1793(12):1811–1818. [PubMed: 19782705]
35. Rangasamy V, Mishra R, Mehrotra S, et al. Estrogen suppresses MLK3-mediated apoptosis sensitivity in ER+ breast cancer cells. Cancer research. 2010; 70(4):1731–1740. [PubMed: 20145118]
36. Humphrey RK, Newcomb CJ, Yu SM, et al. Mixed lineage kinase-3 stabilizes and functionally cooperates with TRIBBLES-3 to compromise mitochondrial integrity in cytokine-induced death of pancreatic beta cells. The Journal of biological chemistry. 2010; 285(29):22426–22436. [PubMed: 20421299]
37. Ribeiro PS, Cortez-Pinto H, Sola S, et al. Hepatocyte apoptosis, expression of death receptors, and activation of NF-kappaB in the liver of nonalcoholic and alcoholic steatohepatitis patients. Am J Gastroenterol. 2004; 99(9):1708–1717. [PubMed: 15330907]
38. Garcia-Monzon C, Lo Iacono O, Mayoral R, et al. Hepatic insulin resistance is associated with increased apoptosis and fibrogenesis in nonalcoholic steatohepatitis and chronic hepatitis C. J Hepatol. 2011; 54(1):142–152. [PubMed: 20888662]
39. Olefsky JM, Glass CK. Macrophages, inflammation, and insulin resistance. Annu Rev Physiol. 2010; 72:219–246. [PubMed: 20148674]
40. Osborn O, Olefsky JM. The cellular and signaling networks linking the immune system and metabolism in disease. Nature medicine. 2012; 18(3):363–374.
41. Chen LL, Ye HY, Zhao XL, Miao Q, Li YM, Hu RM. Selective Depletion of Hepatic Kupffer Cells Significantly Alleviated Hepatosteatosis and Intrahepatic Inflammation Induced by High Fat Diet. Hepato-Gastroenterology. 2012; 59(116):1208–1212. [PubMed: 22328286]
42. Han MS, Jung DY, Morel C, et al. JNK expression by macrophages promotes obesity-induced insulin resistance and inflammation. Science. 2013; 339(6116):218–222. [PubMed: 23223452]
43. Kant S, Swat W, Zhang S, et al. TNF-stimulated MAP kinase activation mediated by a Rho family GTPase signaling pathway. Genes Dev. 2011; 25(19):2069–2078. [PubMed: 21979919]
44. Sharma M, Gadang V, Jaeschke A. Critical role for mixed-lineage kinase 3 in acetaminophen-induced hepatotoxicity. Molecular pharmacology. 2012; 82(5):1001–1007. [PubMed: 22918968]

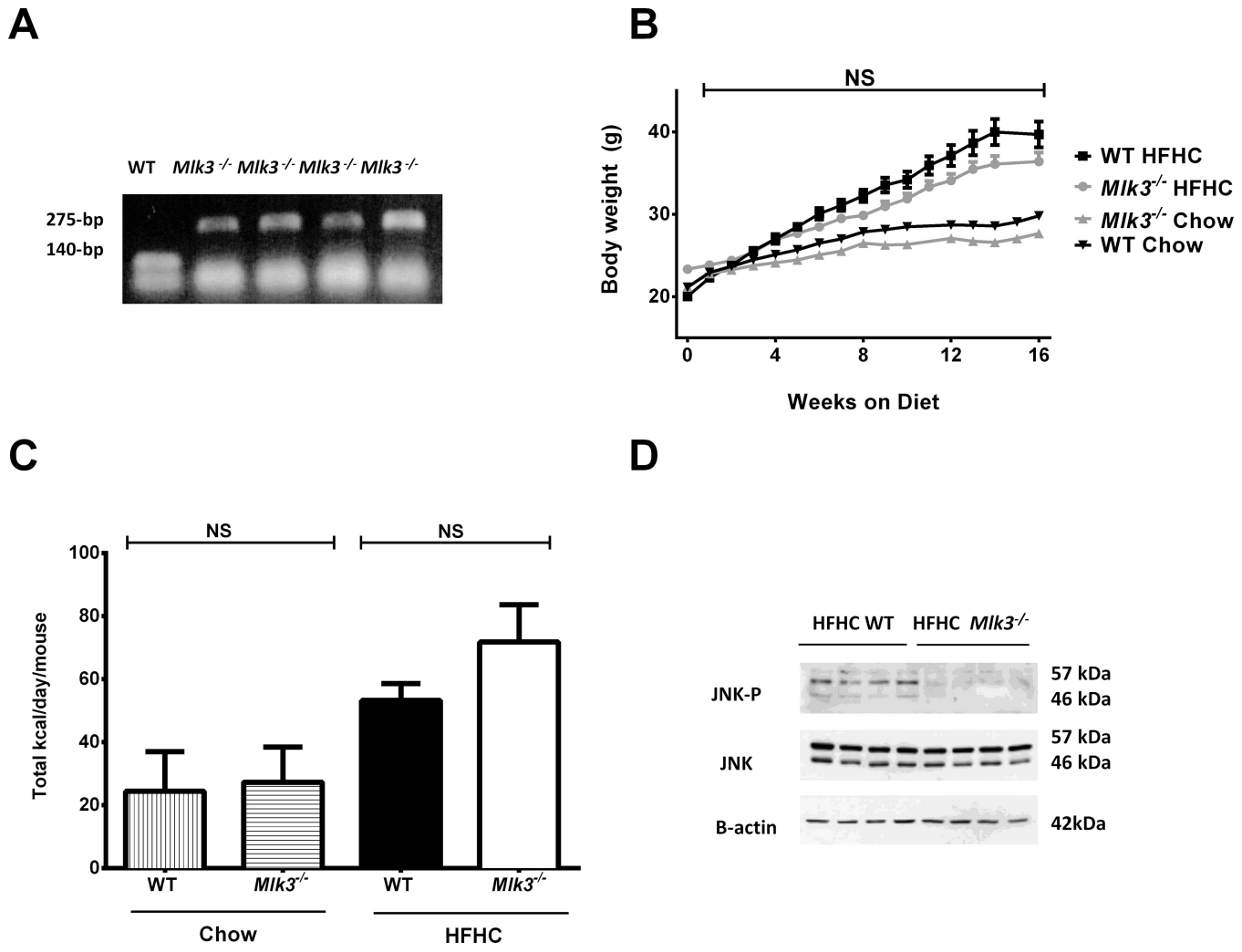

Figure 1. *Mlk3*$^{-/-}$ mice are protected against high fat high carbohydrate (HFHC) diet-induced JNK activation

(A) Genomic DNA isolated from wild type (WT), and mixed lineage kinase 3 (*Mlk3*)$^{-/-}$ mice was examined by polymerase chain reaction (PCR) analysis. (B) Body weights of WT and *Mlk3*$^{-/-}$ mice on chow and HFHC diet were measured on weekly basis throughout the 16-week period of the study. (C) Total caloric intakes of the WT and *Mlk3*$^{-/-}$ mice on chow and HFHC diet were assessed by food and water quantification over a week. (D) Liver protein extracts were prepared from the HFHC-fed WT and *Mlk3*$^{-/-}$ mice. Immunoblot analyses were performed for phosphorylated C-Jun N-terminal kinase (JNK-P); total JNK, and β-actin were used as control for protein loading. Data represent the mean ± SEM; NS non-significant.

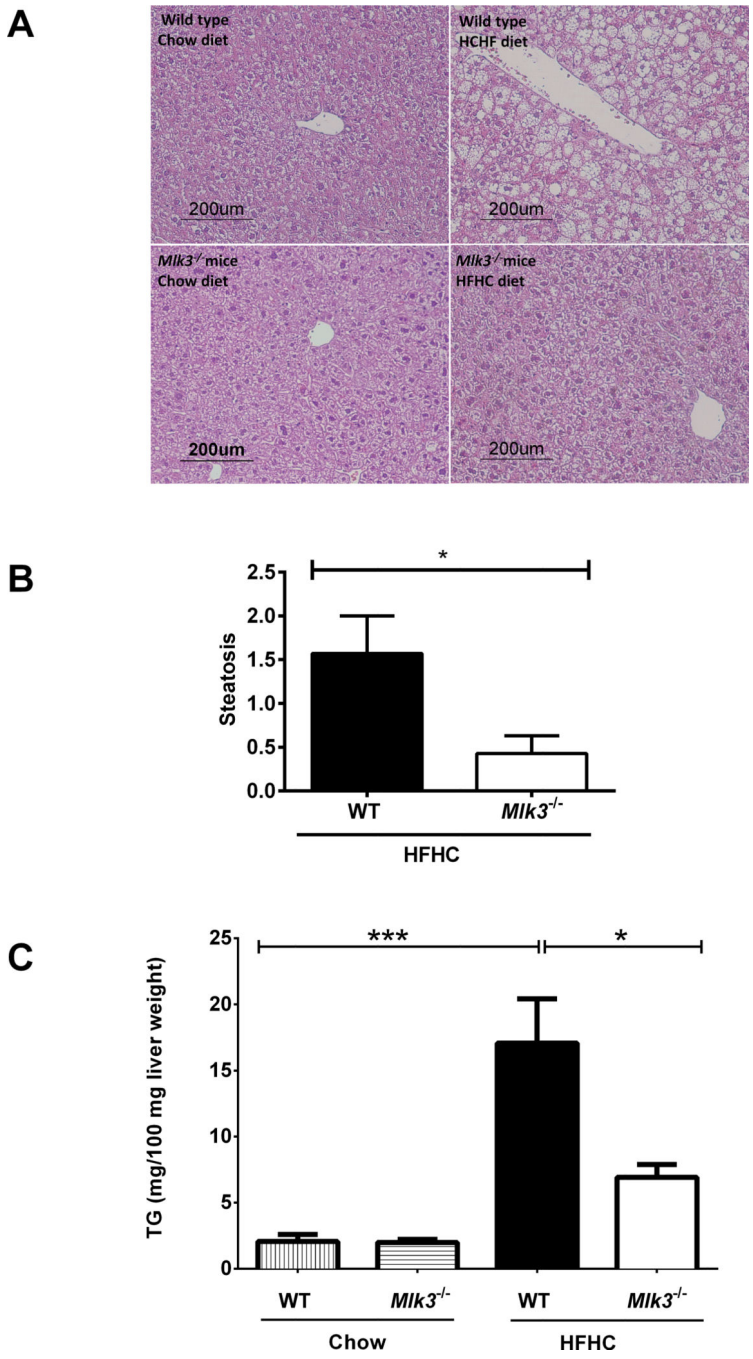

Figure 2. *Mlk3*$^{-/-}$ mice are protected against high fat high carbohydrate (HFHC) diet-induced hepatic steatosis

(A) Fixed liver tissues from wild type (WT) and mixed lineage kinase (*Mlk3*)$^{-/-}$ mice on chow and HFHC diet were stained with hematoxylin & eosin (H&E). (B) The scores for steatosis (0 to 3) were assessed by a pathologist blinded to the identity of the mice; average steatosis scores for the WT and *Mlk3*$^{-/-}$ mice on HFHC diet are indicated in the graph. (C) Concentration of neutral triglycerides (TG) was measured by photometric absorbance based

technique in the liver tissue of WT and *Mlk3*$^{-/-}$ mice on chow and HFHC diet. Data represent the mean ± SEM; *p < 0.05 and ***p < 0.001.

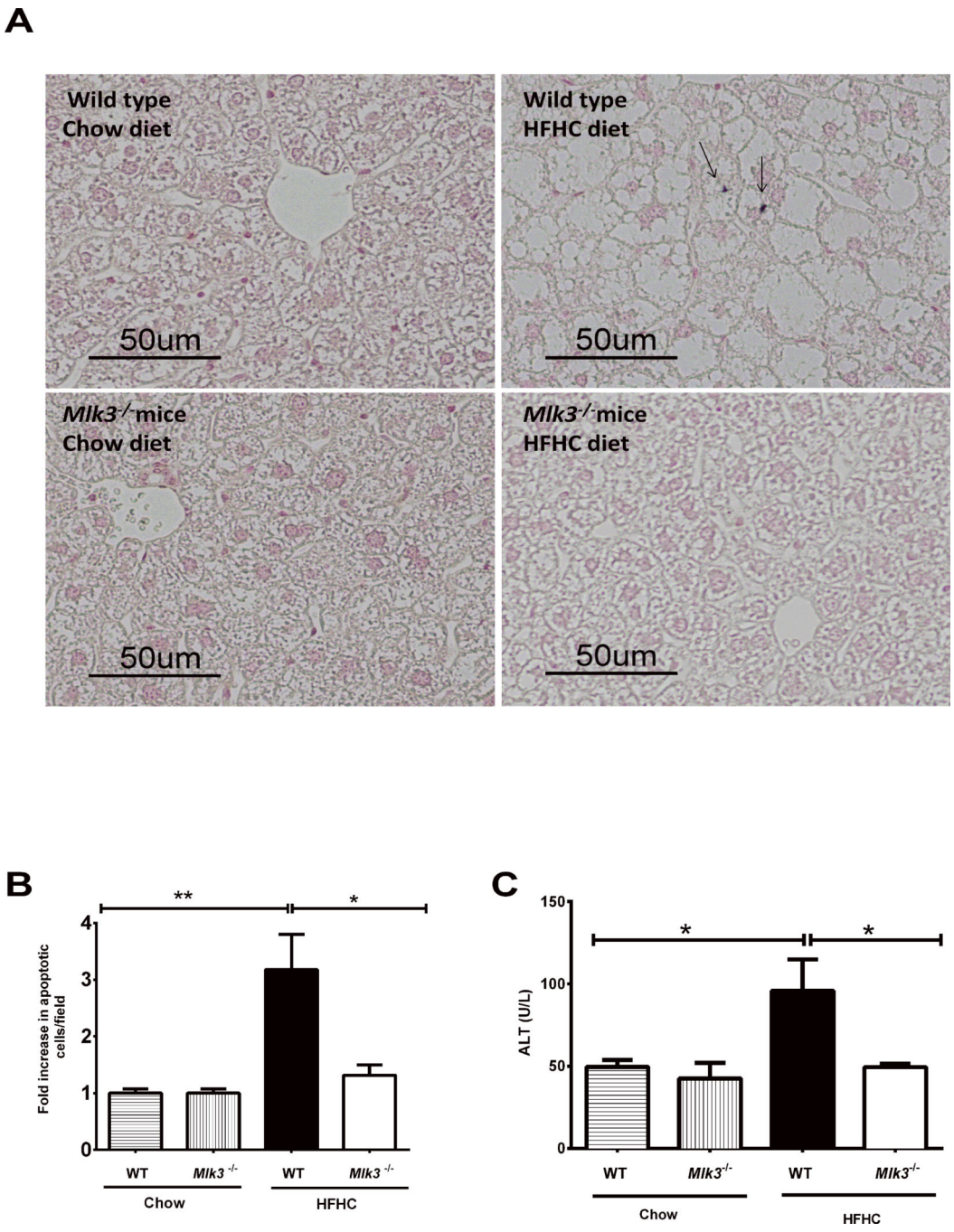

Figure 3. *Mlk3*$^{-/-}$ mice are protected against high fat high carbohydrate (HFHC) diet-induced hepatic apoptosis, and increased alanine aminotransferase (ALT)

(A) Hepatocytes apoptosis was quantified in paraffin-embedded hepatic tissue of 16 week–fed HFHC diet and chow wild type (WT) and mixed lineage kinase (*Mlk3*)$^{-/-}$ mice by labeling DNA strand breaks by the terminal deoxynucleotidyl transferase-mediated deoxyuridine triphosphate nick-end labeling (TUNEL) assay. Apoptotic nuclei were stained brown (black arrows) and quantified by counting nuclei in 10 random 20 × microscopic fields per animal. (B) Apoptotic nuclei were expressed as fold increase over control chow-

fed WT mice, which was arbitrary set at 1. (C) Serum ALT values were measured by photometric absorbance based technique for the WT and *Mlk3*$^{-/-}$ mice on chow and HFHC diet for 16 weeks. Data represent the mean ± SEM; * $p < 0.05$ and **$p < 0.01$.

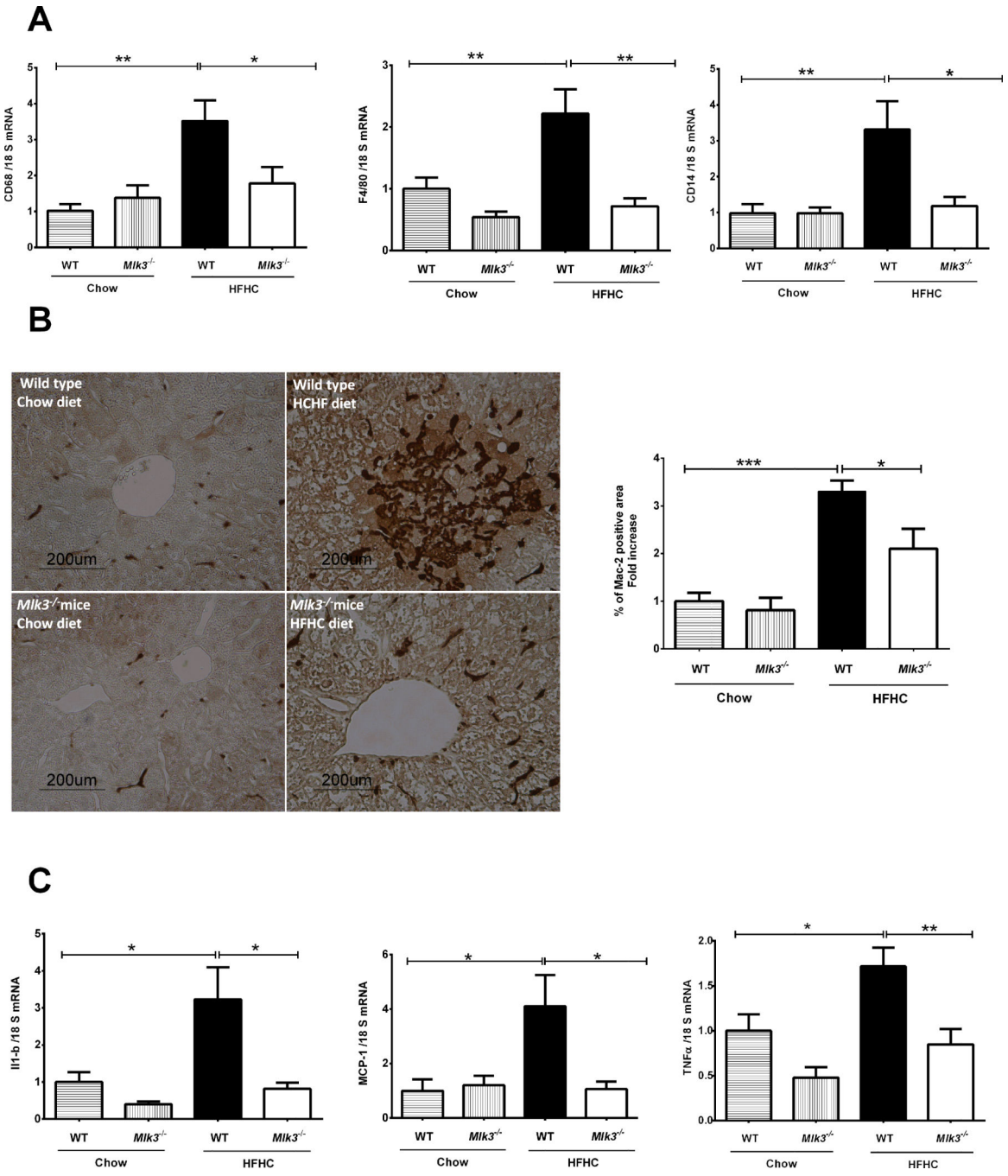

Figure 4. *Mlk3*$^{-/-}$ mice are protected against high fat high carbohydrate (HFHC) diet-induced hepatic macrophage infiltration and activation

(A) Total RNA was extracted from the liver tissue of wild type (WT) and mixed lineage kinase *(Mlk3)*$^{-/-}$ mice on chow and HFHC diet and mRNA expression of macrophage markers cluster of differentiation (CD)68, F4/80 and CD14 were evaluated by real-time polymerase chain reaction (PCR). Fold induction was determined after normalization to 18S mRNA expression. (B) Quantification of macrophage infiltration in the WT and *Mlk3*$^{-/-}$ mice on chow and HFHC diet was done by immunohistochemistry using macrophage

galactose-specific lectin (Mac-2) antibody. Mac-2 immunohistochemical staining was quantified in ten random 20 × microscopic fields per animal by morphometry (KS 400 software, Carl Zeiss). Mac-2 positive area in the liver tissue sections was normalized to control chow-fed WT animals, which was arbitrary set at 1. (C) mRNA expression of cytokines and chemokines related to macrophage activation including interleukin-1 beta (IL-1β), monocyte chemotactic protein-1 (MCP-1), and tumor necrosis factor alpha (TNFα), was assessed by real time PCR, fold induction was determined after normalization to 18S mRNA expression. Data represent the mean ± SEM; *$p < 0.05$, ** $p < 0.01$ and ***$p < 0.001$.

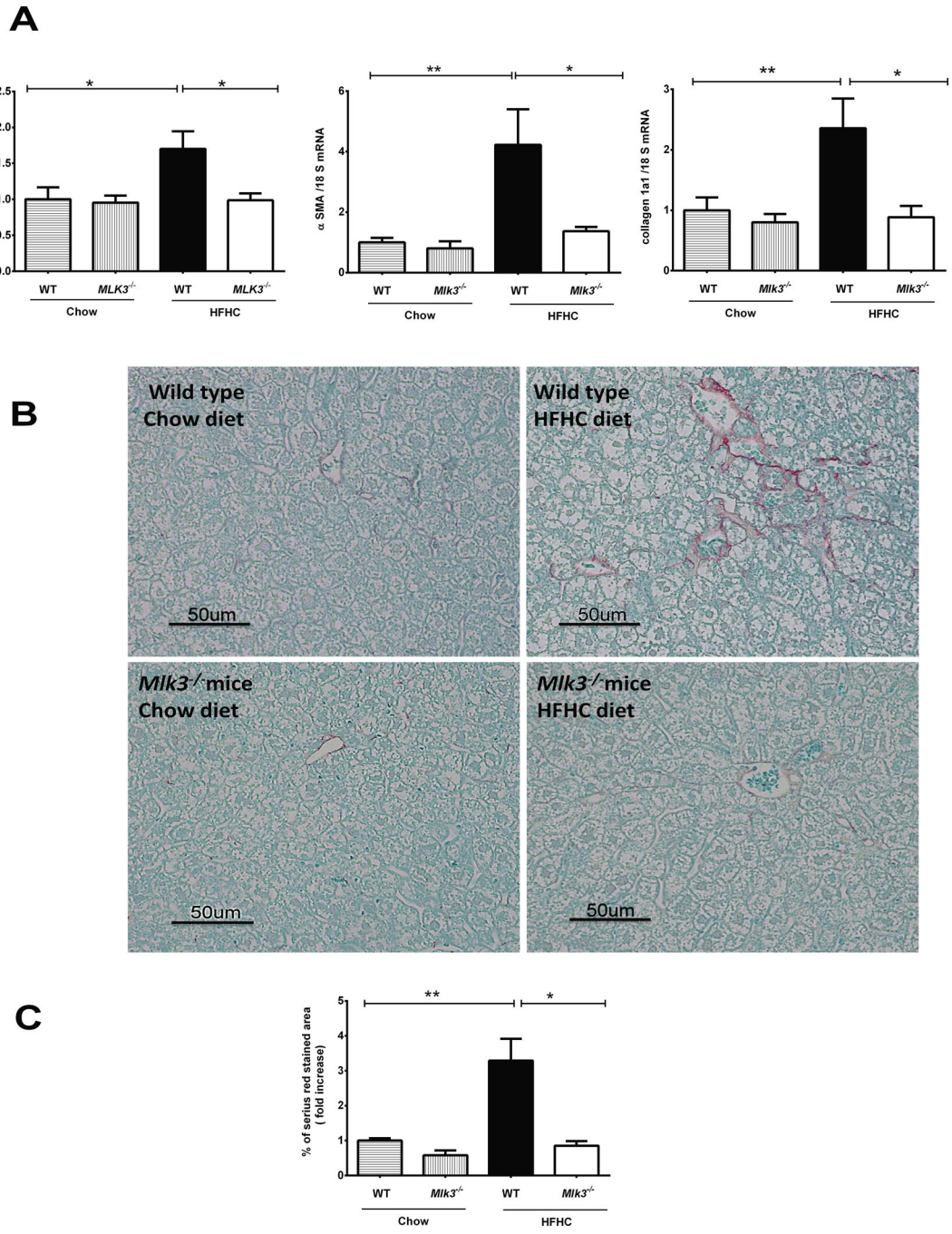

Figure 5. *Mlk3*$^{-/-}$ mice are protected against high fat high carbohydrate (HFHC) diet-induced hepatic fibrosis

(A) Total RNA was extracted from the liver tissue of wild type (WT) and mixed lineage kinase *(Mlk3)*$^{-/-}$ mice on chow and HFHC diet for 16 weeks and profibrogenic markers osteopontin, alpha smooth muscle actin (αSMA), and collagen 1a1 were evaluated by real-time PCR. Fold induction was determined after normalization to 18S mRNA expression. (B) Fixed liver tissue sections from WT and *Mlk3*$^{-/-}$ mice on chow and HFHC diet were stained with Sirius red to detect collagen deposition. (C) Sirius red staining was quantified in ten

random 20 × microscopic fields per animal by morphometry using ImageJ software. Sirius red-stained area in the liver tissue sections was normalized to control chow-fed WT animals, which was arbitrary, set at 1. Data represent the mean ± SEM; * $p < 0.05$ and ** $p < 0.01$.

Table 1

Primer sequences for quantitative real-time PCR

Gene	Forward primer sequence (5'-3')	Reverse primer sequence (5'-3')
αSMA	GTC CCA GAC ATC AGG GAG TAA	TCG GAT ACT TCA GCG TCA GGA
CD14	CTC TGT CCT TAA AGC GGC TTA C	GTT GCG GAG GTT CAA GAT GTT
CD68	TGT CTG ATC TTG CTA GGA CCG	GAG AGT AAC GGC CTT TTT GTG A
Collagen 1a1	GCT CCT CTT AGG GGC CAC T	CCA CGT CTC ACC ATT GGG G
F4/80	ATG GAC AAA CCA ACT TTC AAG GC	GCA GAC TGA GTT AGG ACC ACA A
IL-1β	GCA ACT GTT CCT GAA CTC AAC T	ATC TTT TGG GGT CCG TCA ACT
MCP-1	TTA AAA ACC TGG ATC GGA ACCA	GCA TTA GCT TCA GAT TTA CGG G
Osteopontin	CTC CAT CGT CAT CAT CAT CG	TGC ACC CAG ATC CTA TAG CC
TNFα	CCC TCA CAC TCA GAT CAT CTT CT	GCT ACG ACG TGG GCT ACA G
18S	CGC TTC CTT ACC TGG TTG AT	GAG CGA CCA AAG GAA CCA TA